Synthetic Metals 253 (2019) 62–72

Contents lists available at ScienceDirect

Synthetic Metals

journal homepage: www.elsevier.com/locate/synmet

Redox activity of selenocyanate anion in electrochemical capacitor application

Paulina Bujewska, Barbara Gorska, Krzysztof Fic*

Poznan University of Technology, Institute of Chemistry and Technical Electrochemistry, Berdychowo 4, 60965 Poznan, Poland

ARTICLE INFO

Keywords:
Electrochemical capacitors
Redox-active electrolytes
Selenocyanates
Aqueous electrolyte
Energy storage
Carbon electrodes

ABSTRACT

In this work, we report on the performance of carbon-based electrochemical capacitors operating in an aqueous solution of potassium selenocyanate (KSeCN) as redox active electrolyte, applied for capacitance and energy enhancement. The source of faradaic contribution is pseudohalide anion, $SeCN^-$, demonstrating reversible redox reaction on the positive electrode. Since the standard potential of $SeCN^-/(SeCN)_2/(SeCN)_3^-$ is close to the $I^-/I_2/I_3^-$ redox couple, the capacitor demonstrates similar hybrid operation. With cost-effective stainless steel (SSt) current collectors, the system displays high capacitance 43 $F{\cdot}g^{-1}$ (0.5 $A{\cdot}g^{-1}$) and performs at 1.4 V (1 $A{\cdot}g^{-1}$) for 9 000 cycles with 90% capacitance retention.

1. Introduction

Electrochemical capacitors (ECs), also called supercapacitors or ultracapacitors, are energy storage devices demonstrating moderate energy density, extremely short charging/discharging time and high power [1,2]. The application span of ECs covers large-scale and heavy-duty applications such as stabilization of conventional power grids (induced by fluctuations in electricity production/consumption) [3,4]. ECs can also greatly support the regenerative braking systems in “green” vehicles, claimed to reduce fossil fuel consumption and greenhouse gases emission. Besides large scale applications, capability for high power rates makes their application in smart-technology devices attractive as well, since their presence shortens the charging time of portable equipment from hours to minutes or seconds [5,6].

Although various constructions and technologies of ECs have been developed to date [7–20], electric double-layer capacitors (EDLCs) are the original concept and are still the subject of dynamic development. The advantage of EDLCs’ charging performance, in preference to the batteries, originates from the difference between physical and chemical mechanisms responsible for charge storage process. This substantial difference stays at the origin of various application fields for electrochemical capacitors and batteries. Furthermore, it explains why the context of competition for power/energy densities between these two technologies is non-reasonable.

In principle, electric double-layer capacitors exploit fast, physical electrostatic attractions of ions from the electrolyte onto the electrode surface. Such interfacial organization is called the electric double-layer (EDL) and is known since more than a century. Of course, the physical nature of that kind of interaction implies the "modest" energy density stored in EDLCs. However, one should be aware, that the energy accumulated in that way can be delivered very quickly (up to seconds) since no chemical or electrochemical reaction is involved in the storage mechanism. Furthermore, no structural changes (theoretically) in the electrode material impose the excellent cyclability (up to 1 000 000 charging/discharging cycles).

Another mechanism introduced to electrochemical capacitor technology exploits the redox reactions (i.e., chemical conversion) of electro-active components in the electrode or electrolyte bulk. Unfortunately, these processes are time-limited either by the reaction kinetics or diffusion of reacting species [21] and aggravates the power rate remarkably. However, incorporation of redox-based processes to the energy storage mechanisms improves the energy density and moves the capacitors closer to the conventional batteries – with all their advantages and drawbacks (such as limited cyclability).

As already mentioned, the capacitive energy storage is not a “novel”, “extraordinary” and “outstanding” concept. Electrochemical capacitors might be thus considered as the next generation of conventional dielectric capacitors, where the low-surface electrodes (up to 10 $m^2{\cdot}g^{-1}$) have been substituted by porous materials with well-developed surface area (up to 2200 $m^2{\cdot}g^{-1}$), as the capacitance C increases linearly with the electrode/electrolyte interface surface (until “saturation” point, where the screening effect of the thin pore walls starts to play a negative role) [22–28].

* Corresponding author.
E-mail address: krzysztof.fic@put.poznan.pl (K. Fic).

https://doi.org/10.1016/j.synthmet.2019.04.024
Received 7 February 2019; Received in revised form 13 April 2019; Accepted 24 April 2019

$$C = \frac{\varepsilon S}{d} \quad (1)$$

Since the increase of EDLCs' capacitance has been achieved mostly by the development of the electrode/electrolyte interface, the application of electrodes based on high surface area activated carbons (ACs) became a leading technological strategy [29–40]. These materials are well-conductive, light-weight, eco-friendly and cost-effective [1,2,37,39–47]. It is worth noting here that caution shall be taken when the specific surface area and corresponding pore size distributions are reported and correlated with electrochemical data. It should be clearly stated that the BET equation is a powerful tool for estimation of the specific surface area, however, for highly microporous materials it might reflect confusing and quite often overestimated results. Only the combination of several techniques (gas adsorption, immersion calorimetry) allows for a reliable determination of that value [26,48–51]. Moreover, the specific surface area cannot be considered as the electrochemically accessible one, since the wettability of carbon (and porous materials) is usually limited. In this aspect, the specific capacitance of the EDL, ranging from 20 to 50 $\mu F \cdot cm^{-2}$, could serve as a controlling factor [42].

Taking into account the formula for the total energy stored in a capacitor, *E*:

$$E = \frac{1}{2} C_{device} U^2 \quad (2)$$

where *C* is the capacitance of the device (not the electrode), *U* is the max. Operating voltage, it appears that the kind of electrolyte applied plays an important role.

In this place, it is worth mentioning that one must not apply Eq. (2) if the *C* value is for a single electrode. In the simplest case, if the specific energy is calculated for the symmetric system (i.e., composed of two identical electrodes), one should apply the following formula:

$$E = \frac{1}{8} C_{electrode} U^2 \quad (3)$$

as the specific capacitance of symmetric system, where the capacitance of positive and negative electrode is described by Eqs. (4a–d):

$$\frac{1}{C_{device}} = \frac{1}{C_{+\,electrode}} + \frac{1}{C_{-\,electrode}} \quad (4a)$$

$$C_{+electrode} = C_{-electrode} = C_{electrode} \quad (4b)$$

$$\frac{1}{C_{device}} = \frac{1}{C_{electrode}} + \frac{1}{C_{electrode}} = \frac{2}{C_{electrode}} \quad (4c)$$

$$C_{device} = \frac{1}{2} C_{electrode} \quad (4d)$$

If $C_{electrode}$ is given as a specific capacitance ($F \cdot g^{-1}$), resulting in specific energy (in $J \cdot g^{-1}$), one must take into account the mass of two electrodes (i.e., divide by 2) in a full device, therefore:

$$E = \frac{1}{2}\left(\frac{1}{2} \cdot \frac{1}{2} C_{electrode}\right) U^2 \quad (4e)$$

so gives Eq. (3). It should be clearly stated that Eq. (4e) should be used for approximate estimation of the specific energy accumulated in the device if the specific capacitance of a single electrode in a symmetric system is known. One cannot use Eq. (3) for the calculations concerning asymmetric systems (i.e., built from electrodes of different capacitance) or hybrid systems. Furthermore, one should be aware that the results from three-electrode experimental set-up do not allow for reliable energy estimation. Indeed, energy is stored in two electrodes. Despite this is a quite intuitive conclusion, there are still many papers reporting the specific energy for the electrodes. Such practice, although mathematically possible, does not have any practical meaning.

Commercial ECs operate most often with organic electrolytes or ionic liquids [52]. Aprotic medium ensures high energy density because of the high operating voltage values, namely 2.5-3.0 V for organic solvents based on acetonitrile and propylene carbonate or 3.0-3.5 V for ionic liquids [1,2,17,18,20,39,53–66]. However, the manufacturing of ECs with organic electrolyte requires ultra-dry components (electrodes and electrolytes), assembled in an inert atmosphere (oxygen and moisture-free). Hence, the initial cost of the investment is relatively high.

In contrast, aqueous electrolytes are a low-cost and eco-friendly alternative. Furthermore, conductivity of water-based formulations is noticeably higher than for organic ones. However, the capacitors operating with aqueous electrolytes suffer from poor energy density imposed by restricted operational voltage. The reason for that is electrochemical stability of water (1.23 V). In practical terms, the maximum voltage differs with electrolyte pH; for acidic (H_2SO_4) and alkaline (KOH) aqueous electrolytes the voltage does not exceed 1.0 V [67]. Interestingly, for pH neutral electrolytes, the max. voltage is remarkably higher: 1.6 V for the capacitor operating with 0.5 $mol \cdot L^{-1}$ Na_2SO_4 [68,69] solution or even 2.0 V for 1 $mol \cdot L^{-1}$ Li_2SO_4 solution with gold current collectors [70,71]. Commercially applicable stainless steel (SSt) current collectors allow the maximum voltage of 1.5 V for 1 $mol \cdot L^{-1}$ Li_2SO_4 to be reached [72]. In this aspect, one should pay attention that the kind of current collector has a remarkable impact on the overall ECs performance and caution shall be taken during the selection of the material for that part of the device. In a long-term perspective, corrosion-related issues start to impede the overall performance of the device [72–80].

Despite the voltage of the devices operating with pH-neutral electrolytes is relatively high, the energy delivered is not satisfactory. As a consequence of Eq. (2), another strategy for energy improvement is focused on the "enhancement" of the capacitance by the contribution of capacitive faradaic current (so-called pseudocapacitance) and/or non-capacitive faradaic current (redox) [81–85]. Recently, the "pseudocapacitance" term is largely overused, mostly for the materials demonstrating typical battery-like performance. In the original concepts [86–89], pseudocapacitive materials included selected transition metal oxides such as RuO_2, MnO_2 [90] and conducting polymers [91]. Detailed mathematical description of the pseudocapacitance effect, followed by insightful discussion has been presented in [92,93].

It has to be noted, that "pseudocapacitance" term concerns the electrode, not the device; hence, the term "pseudocapacitor" is not recommended. Detailed discussion on the pseudocapacitive effects, accompanied by the list of good practices in reporting the electrochemical data are provided elsewhere [82,94].

Although non-capacitive, the contribution from redox activity of the electrolyte solution appears to be an interesting idea. Primarily introduced for iodide-based electrolytes [95–97], the concept of redox-active electrolytes is recently developed in several ways:

1) by their impregnation in AC-based electrodes [98–100],
2) by grafting electroactive species on activated carbons applied as electrode material [101–107],
3) formulation of new redox-active electrolytes [95,96,108–113].

The most dominant redox-couples, considered in many reports, are quinones (Scheme 1) with ketone functionalities reduced to hydroxyls, preferably in two-electron reaction. This group includes various monocyclic quinones, listed below, together with their reduced forms:

1) 1,4-benzoquinone (Q, **1a**) /1,4-dihydroxybenzene (hydroquinone, HQ, **1b**) characterized by redox-favored substituent positions [108–110], its less active isomer 1,2-benzoquinone (**3a**) /1,2-dihydroxybenzene (catechol, **3b**) [103,110] and thermodynamically impeded 1,3-benzoquinone diradical (**2a**) /1,3-dihydroxybenzene (resorcinol, **2b**) [110];
2) substituted quinones like tertachloroquinone (TCQ, **4a**) /tetrachlorohydroquinone (TCHQ, **4b**) [99] or dibromoquinone (**5a**) /dibromohydroquinone (**5b**) [110].

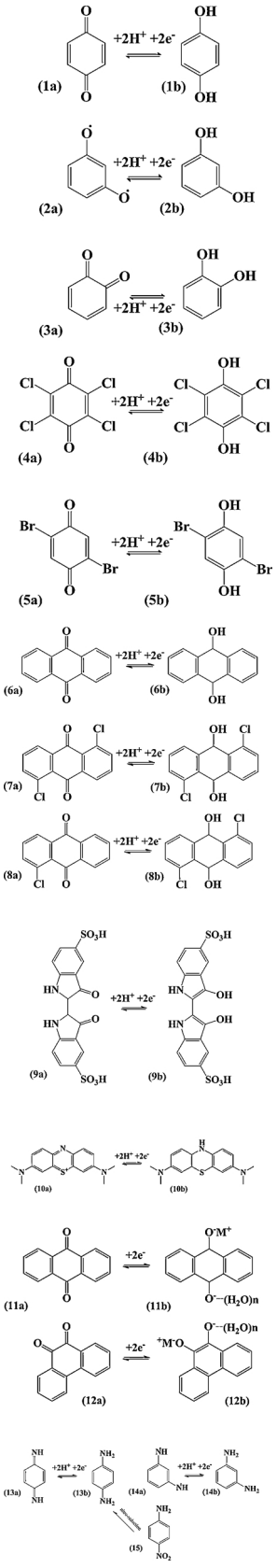

Scheme 1. Redox activity of various organic molecules.

Tricyclic quinone derivatives, anthraquione (AQ, **6a**) /dihydroxyanthracene (DHA, **6b**) [99,101,102] are also popular, as well as their substituted analogues: 1-chloroantraquinone (**7a**) /1-chlorodihydroxyanthracene (**7b**) [104], 1,5-dichloroanthraquione (DCAQ, **8a**) /1,5-dichlorohydroxyantraquinone (DCHAQ, **8b**) [99].

These organic compounds were reported to require acidic electrolyte since protons are necessary for the reaction [110]. The same medium is required for triggering electro-activity of redox-indicators like indigo carmine (**9a, b**) or methylene blue (**10a, b**) [114,115]. The Q/HQ redox couple is inactive in neutral electrolytes, but it demonstrates redox activity in the alkaline medium as well (NaOH) [110].

The application of alkaline solution (KOH) was reported for AQ/DHA, (**11a, b**) [106] and 9,10-phenanthrenequinone (PQ, **12a, b**) [107] as well for *p*- and *m*-phenylenediamine additives (PPD **13a, b** and MPD **14a, b**; respectively) [116,117] or *p*-nitroaniline undergoing nitro-reduction to PPD (**15**) [100]. A serious disadvantage of these compounds, especially in their oxidized forms, is limited solubility in water (ketone groups are less hydrophilic than hydroxyl ones) or poor wetting of electrode by aqueous electrolyte if impregnated in electrodes or grafted on ACs. For these reasons, the attention has been drawn to the inorganic molecules and compounds, such as cerium incorporated salts like Ce2(SO4)3 [118] or (NH4)2Ce(NO3)6 [119]. However, their usage imposes the retention of toxic metals in used and disposed devices.

Another option is the application of inorganic salts containing halide anions: bromides [120,121] and iodides [122–126]. Their electroactivity is described by the Eq. (5a)–(6d):

$$2Br^- \leftrightarrow Br_2 + 2e^- \quad (5a)$$

$$Br^- + Br_2 \leftrightarrow Br_3^- + 2e^- \quad (5b)$$

$$2Br_3^- \leftrightarrow 3Br_2 + 2e^- \quad (5c)$$

$$Br_2 + 6H_2O \leftrightarrow 2BrO_3^- + 12H^+ + 10e^- \quad (5d)$$

$$3I^- \leftrightarrow I_3^- + 2e^- \quad (6a)$$

$$2I^- \leftrightarrow I_2 + 2e^- \quad (6b)$$

$$2I_3^- \leftrightarrow 3I_2 + 2e^- \quad (6c)$$

$$I_2 + 6H_2O \leftrightarrow 2IO_3^- + 12H^+ + 10e^- \quad (6d)$$

It is clearly seen that they differ only by the standard potentials $Br^-/Br_2/Br_3^-$ with $E^\circ = 1.07$ V vs. $I^-/I_2/I_3^-$ with $E^\circ = 0.54$ V. Since bromide might provoke corrosion on stainless steel, iodide-based formulations are the most popular to date and have been applied as:

1) electrolyte itself with the EC voltage of 0.8 V [95,112,120] or 1.2 V [110,123];
2) additive to acidic medium (H_2SO_4) U = 0.8 V [111,127];
3) additive to neutral electrolyte, with U = 0.8 V [111] or 1.6 V [124];
4) additive to alkali medium U = 1.6 V (KOH) [113].

The application of KOH solution as supporting electrolyte was proven to provoke oxidation of I^- to IO_3^- or IO_4^- as an alternative redox pathway instead of conventional $I^-/I_2/I_3^-$ reaction pathway (Eq. (5d)) [113]. Simultaneously, the operational voltage has been extended to 1.6 V [122,128,129].

More advanced strategy exploits separated electrolytes referred to as catholyte /anolyte, e.g., NaOH and I_3^-/I^- [122] or $Mg(NO_3)_2$ and I_3^-/I^- [125] or the vanadium/vanadyl [126] and I_3^-/I^-. In the case of bromine, mixed redox couples, e.g., Br_3^-/Br^- from KBr and 1,1'-dimethyl-4,4'-bipyridinium (methyl viologen) dichloride ($MVCl_2$) [120] or 1,1'-diethyl-4,4'-bipyridinium (ethyl viologen) dibromide [121] were successfully applied (Scheme 2).

Recently, our research group implemented thiocyanate/thiocyanogen ($SCN^-/(SCN)_2$) redox-couple [130] as an interesting alternative to typical halide anions. For instance, KSCN is an inexpensive salt, highly soluble in water, allowing for EC safe operation at 1.6 V on stainless steel (SSt) current collectors and providing a faradaic contribution on a positive electrode. Thiocyanate anion itself is classified as

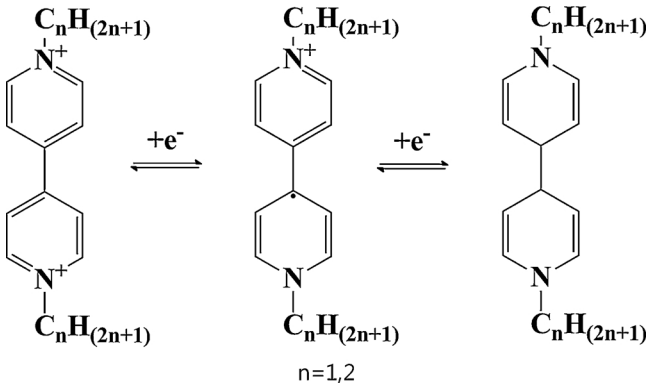

Scheme 2. Redox activity of 1,1'-diethyl-4,4'-bipyridinium [120,121].

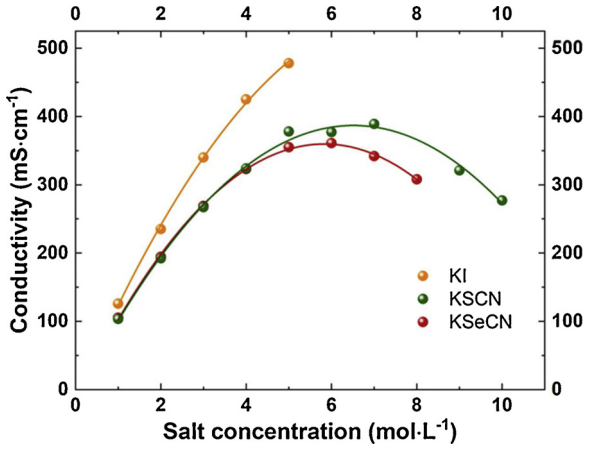

Fig. 1. Conductivity for the aqueous solutions of KI, KSCN, and KSeCN vs. salt concentration.

Table 1
Conductivity and pH measured for 2 mol·L^{-1} KSeCN, KSCN and KI electrolytes.

	2 mol·L^{-1} KSeCN	2 mol·L^{-1} KSCN	2 mol·L^{-1} KI
Conductivity (mS·cm^{-1})	194	192	228
pH	10.33	6.48	6.66
E_{H2} vs. SCE (V)	−0.85	−0.62	−0.63
E_{O2} vs. SCE (V)	+0.38	+0.61	+0.60

a pseudohalide; the name owes to its physicochemical and electrochemical properties imitating genuine halides.

In this paper we propose the application of selenocyanate/selenocyanogen ($SeCN^-/(SeCN)_2$) redox-couple. This redox couple is a very effective alternative to various redox mediators for dye-sensitized solar cells (DSSCs) such as halogens (X-X: I_3^-/I^- and Br_3^-/Br^-), pseudohalogens (Ps-Ps: $SCN^-/(SCN)_2$) or combined ones (XPs) [131–138].

$$6SCN^- \leftrightarrow 2(SCN)_3^- + 4e^- \quad (7a)$$

$$2(SCN)_3^- \leftrightarrow 3(SCN)_2 + 2e^- \quad (7b)$$

$$(SCN)_2 + SCN^- \leftrightarrow (SCN)_3^- \quad (7c)$$

$$6SeCN^- \leftrightarrow 2(SeCN)_3^- + 4e^- \quad (8a)$$

$$2(SeCN)_3^- \leftrightarrow 3(SeCN)_2 + 2e^- \quad (8b)$$

$$(SeCN)_2 + SeCN^- \leftrightarrow (SeCN)_3^- \quad (8c)$$

Considering molecular structure, the sulfur atom in the SCN^- anion is replaced by more reactive selenium in $SeCN^-$. Therefore, in terms of electrochemistry, $SeCN^-/(SeCN)_2$ redox couple is expected to display similar electrochemical activity to the $SCN^-/(SCN)_2$ (Eq. (8a–c)), but at lower formal potentials. According to the literature reports, two current peaks of $SeCN^-/(SeCN)_2/(SeCN)_3^-$ appear during positive scans in the range of 0.2 ÷ 0.35 V vs. SCE (platinum electrode and acetonitrile as supporting electrolyte) [139], or either between −0.064 and −0.18 V vs. Fc/Fc^+ (ferrocene/ferrocenium) [136] or in between +1.3 and +1.6 V vs. Cc^+/Cc (cobaltocenium/cobaltocene) on glassy carbon [134], both in IL ([EMIm][TFSI]). It means that on AC-based electrode, a faradaic contribution from selenocyanates is expected in the potential comparable to $I^-/I_2/I_3^-$.

This report presents the performance of hybrid ECs based on 2 mol·L^{-1} KSeCN aqueous solution. The system demonstrates such operation owing to the low potential of $SeCN^-/(SeCN)_2/(SeCN)_3^-$ redox couple imposing redox reaction on the positive one and EDL on the negative one. The investigated ECs operates at the max. voltage of 1.4 V; the high specific capacitance of the device, i.e., 43 F·g^{-1} at 0.5 A·g^{-1} and long cycle life proven by 90% of capacitance retention after 9 000 cycles are demonstrated.

2. Experimental

Capacitors were assembled in Swagelok® cells made of Teflon®, in two different configurations: typical two-electrode systems and two-electrode systems quipped with the reference electrode. Components of the composite electrodes, i.e., active material – carbon black (black pearls BP2000 by Cabot; 80 wt.%), percolator (conductive carbon black TIMCAL Super C65 by Imerys; 10 wt.%) and binder (polytetrafluoroethylene PTFE by Sigma Aldrich, 60 wt.% dispersion in water, 10 wt.%) were mixed together with ethanol; produced slurry was stirred at 120 °C till solvent evaporation. The obtained dough was then rolled to form a sheet (thickness ca. 300 μm), then electrodes (pellets) with a geometric surface area of 0.785 cm^2 and mass ca. 12–13 mg were punched. The characterization of electrode material was performed by nitrogen adsorption-desorption at 77 K (ASAP 2460, Micromeritics). The Brunauer–Emmett–Teller (BET) equation was used to calculate the specific surface area (1210 m^2·g^{-1}); the pore size distribution was calculated by using two-dimensional non-local density functional theory (2DNLDFT, [140–142]) ($L_0 < 2$ nm = 0.9 nm; $2 < L_0 < 50$ nm = 15 nm), both in details reported elsewhere [130]. Swagelok® cells were assembled with the stainless steel current collectors. In three-electrode (i.e. two-electrode with the reference one) configuration, saturated calomel electrode (SCE) was applied as a reference electrode. Glassy fibrous material (Whatman™ GF/A with 0.26 mm of thickness and 1.6 μm of pore size) was used as a porous membrane (separator).

The electrolyte applied was 2 mol·L^{-1} aqueous solution of potassium selenocyanate (KSeCN, reagent grade, 97%, Sigma Aldrich). The reference electrolytes were 2 mol·L^{-1} KI and KSCN solutions (≥99%, Sigma Aldrich). Conductivity and pH of the electrolytes were measured using Conductometer S230 SevenCompact™ (Mettler Toledo™) with an accuracy ± 0.5% and pH meter S220 SevenCompact™ (Mettler Toledo™) with a relative accuracy ± 0.002 at ambient temperature.

The investigations were performed using the following electrochemical techniques: cyclic voltammetry (CV; scan rates from 10 to 100 mV·s^{-1}), galvanostatic cycling with potential limitation (GCPL; current densities in range of 0.5–10 A·g^{-1}) and electrochemical impedance spectroscopy (EIS; frequencies from 1 mHz to 100 kHz with sinusoidal signal of ± 5 mV·s^{-1}) performed at VMP3 multichannel potentiostat/galvanostat by BioLogic.

Capacitance values were calculated per mass of the active material as follows:

1) from cyclic voltammetry (C_{CV}) based on the equation:

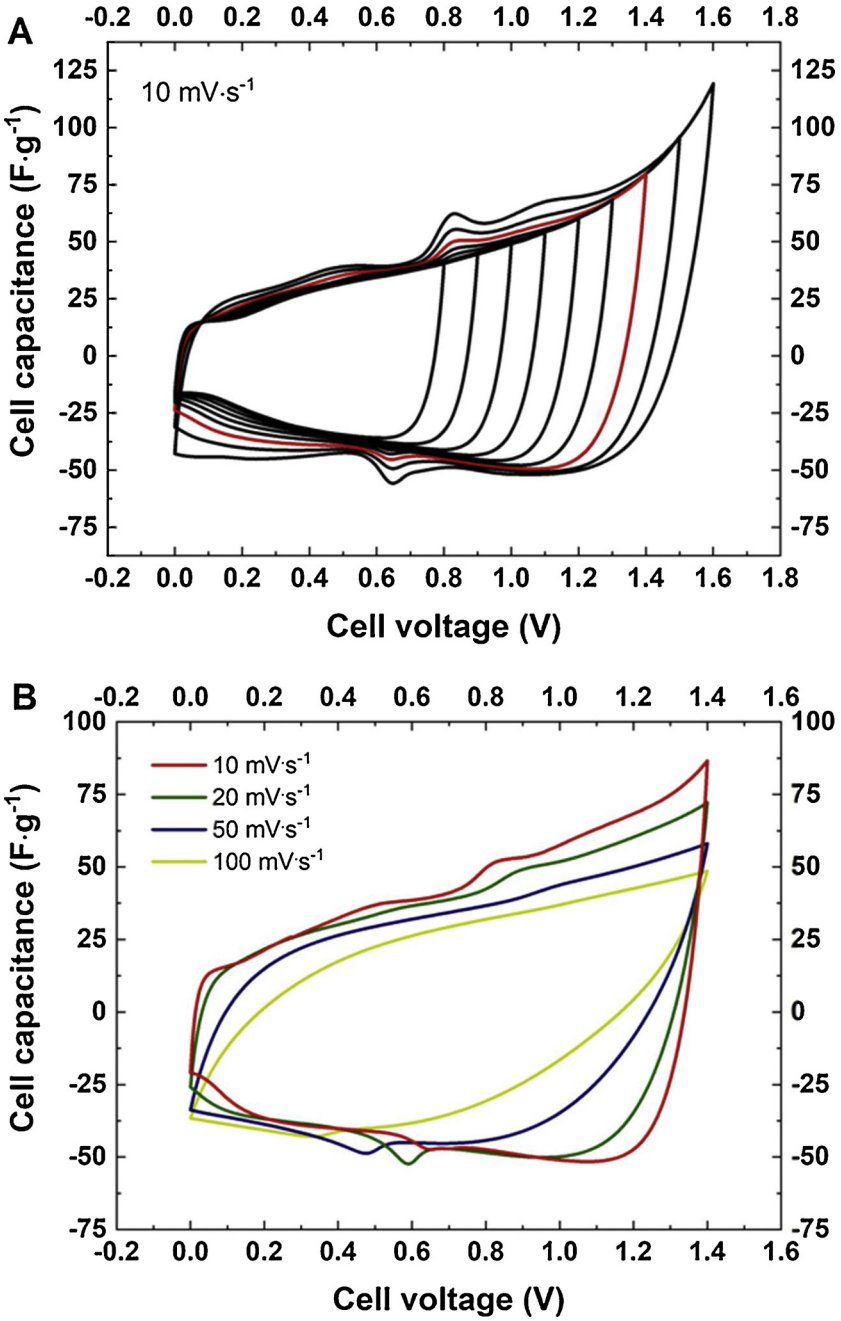

Fig. 2. Cyclic voltammetry profiles for the symmetric capacitor operating in 2 mol·L^{-1} KSeCN solution: (a) gradual voltage increase; (b) cyclic voltammetry profiles for various scan rates.

$$C_{CV} = \frac{I}{\upsilon \cdot m_{act}}$$

1) from galvanostatic charge/discharge (C_{GD}) using the area under the discharge curve (S_{disch}, $V{\cdot}s^{-1}$):

$$C_{GD} = \frac{2 \cdot I \cdot S_{disch}}{U_{max}^2 \cdot m_{act}}$$

1) from impedance spectroscopy (C_{imp}) according to the formula:

$$C_{imp} = \frac{1}{2 \cdot \pi \cdot f \cdot (-Im(Z)) \cdot m_{act}}$$

where *I*– current [A], S_{disch} - the area under the discharge curve [V·s], U_{max} – maximum operating voltage [V], m_{act}– mass of the active material in the device [g], v – scan rate applied [V·s^{-1}], f – frequency [Hz] and *-Im(Z)*– imaginary part of the impedance [Ohm].

All capacitance values reported are expressed per total active mass in the device.

3. Results and discussion

Taking into account the similar formal potentials of $I^-/I_2/I_3^-$ and $SeCN^-/(SeCN)_2/(SeCN)_3^-$ redox systems, the ECs based on KSeCN-redox electrolytes were expected to display performance alike to the system based on the electrolyte with iodide salts. Therefore, considering findings of Frackowiak et al. [112], who evaluated the influence of iodide salt concentration on the operation metrics of ECs, and found that the highest capacitance, efficiency, and reversibility of the process were recorded for 2 mol·L^{-1} sodium iodide solution, the same concentration

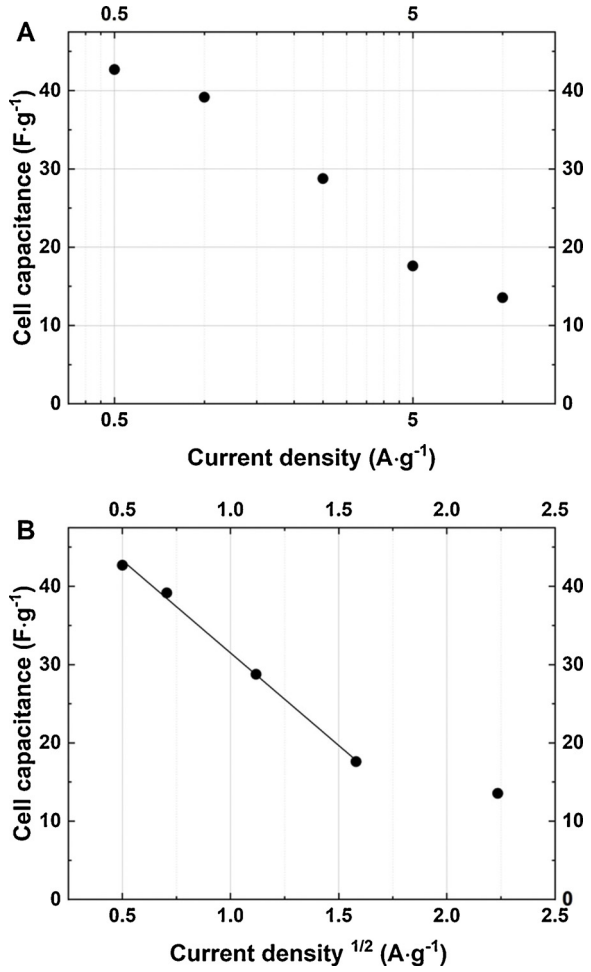

Fig. 3. Capacitance vs. (a) current density (b) square root of current density for the EC operating with 2 mol·L^{-1} KSeCN.

Table 2
Energy and coulombic efficiency of ECs operating is 2 mol·L^{-1} KSeCN.

Current density (A·g^{-1})	0.5	1	2.5	5	10
Energy efficiency (%)	70	72	63	47	32
Coulombic efficiency (%)	86	92	100	100	100*

* in certain cases, the coulombic efficiency exceeded 100%, indicating additional, parasitic reactions in the system, with no practical meaning.

(2 mol·L^{-1}) of KSeCN was selected for our study.

3.1. Conductivity and pH measurements

Conductivity and pH of aqueous electrolytes are key parameters for their application in ECs. Conductivity is considered to control the ion transport rate, which is essential for diminishing the ohmic drop and device response time. pH influences the potential of electrolyte oxidation and reduction (electrochemical stability window) and the profile of electrode potentials adapted by the EC itself.

Conductivity of KSeCN solutions as well as its analogues, added for comparative purposes (KSCN and KI), are presented in Fig. 1 and for selected concentrations in Table 1.

2 mol·L^{-1} KSeCN and KSCN solutions display almost the same conductivity (194 vs. 192 mS·cm^{-1}), whereas the conductivity of KI electrolyte is considerably higher (228 mS·cm^{-1}). In fact, these values are superior to the conductivity of so called-neutral salts, e.g., alkali metal sulfates. One of the features imposing advantageous conductivity of KSeCN and KSCN is the lack of extensive hydrogen bonding in contrast to the sulfates or other oxoacid-derived salts. It results from the cyano-group (−C≡N) in the anion structure restricting the creation of H-bonds between themselves. Furthermore, the discrepancy between salts containing pseudohalides (KSeCN and KSCN) and halides (KI) reflects the distinct size of the polyatomic pseudohalides and monoatomic halides as well as their different solvation characteristics.

It should be noted that the pH of "neutral" electrolytic solutions is not always absolutely "neutral" (i.e., equal to 7 on the pH scale) and reflects the relative strength of acid and base of which they were formed. Although selenocyanate anion shares characteristics of thiocyanate or iodide ones, the selenocyanic acid, HSeCN, is classified as a weak acid in contrast to its analogs: thiocyanic acid (HSCN, pKa = 1.1 at 20 °C) or hydrogen iodide (HI, pKa = −9.5). Accordingly, it is reflected in experimental pH values of their 2 mol·L^{-1} solutions (Table 1): close to 7, indicating neutral character for KI and KSCN electrolytes, being in contrast to 10.33 for KSeCN one. Taking into account the Nernst equation, the higher the pH, the lower the potential of oxygen (E_{O2}) and hydrogen evolution (E_{H2}). Accordingly, E_{O2} and E_{H2} of KSeCN solution are shifted towards lower values (Table 1) in comparison to KSCN and KI ones.

In this case, the positive electrode is protected against oxidation, since it is supposed to operate below E_{O2}. Additionally, as claimed in our previous report, [143] alkaline solution is expected to shift the potential of negative electrode towards lower values, near E_{H2}, which might have a protective impact for long-term capacitor performance.

3.2. Electrochemical measurements

Fig. 2 presents cyclic voltammograms of the symmetric system operating with 2 mol·L^{-1} KSeCN solution. Initially, the maximum operating voltage is determined by gradually expanding vertex voltage from 0.8 V to 1.6 V, with a shift of 100 mV (Fig. 2a). As expected, the shape of the obtained cyclic voltammograms (CV) is substantially similar to the CV profiles characteristic of iodide salts-based electrolytes [95,112]. During initial voltage step (0.8 V), a rectangular shape typical of the EDL charging is observed in a very narrow voltage range, from 0 to 0.2 V. For higher voltages, the voltammogram is modified because of the electro-activity from $SeCN^-/(SeCN)_2$ redox couple. Non-capacitive current appears at significantly lower voltages in comparison to KSCN based electrolytes [130] illustrating the difference in formal potentials of these two pseudohalides. Along the increasing voltage, the EDL part diminishes, reflecting the self-adjustment of electrode potentials in order to balance the charge accumulated in both electrodes. The optimum voltage is achieved at 1.4 V (red curve). At higher cell voltages (above 1.4 V), the current recorded increases considerably, and some additional/parasitic peaks are observed at 0.7 ÷ 0.9 V during charging and 0.7 ÷ 0.6 V during discharging.

Holding the maximum voltage of 1.4 V, the effect of scan rate (10–100 mV·s^{-1}) on charge propagation is determined (Fig. 2b). For moderate scan rates (10 and 20 mV·s^{-1}) good charge propagation is retained, while the capacitance values are high (87 F·g^{-1} and 72 F·g^{-1}, respectively). At higher scan rates (50 and 100 mV·s^{-1}) the CV profiles become more resistive; this indicates deteriorated charge propagation and aggravates the capacitance values. Moreover, the characteristic shape originating from the faradaic contribution diminishes because the scan rate is too fast for charge transfer reactions. Despite the high conductivity of the electrolyte, the presence of dimers and trimers limits the ion diffusion and charging efficiency at high regimes.

Corresponding results were obtained using the galvanostatic technique (current density range: 0.5–10 A·g^{-1}). Fig. 3a presents a variation of capacitance values vs. current load applied. The capacitance retention is better pronounced at moderate values (0.5 and 1 A·g^{-1} with 43 F·g^{-1} and 39 F·g^{-1}, respectively) than at higher current loads. The tendency can be evaluated using the plot representing capacitance vs. current density square root (Fig. 3b). It allows estimation whether the

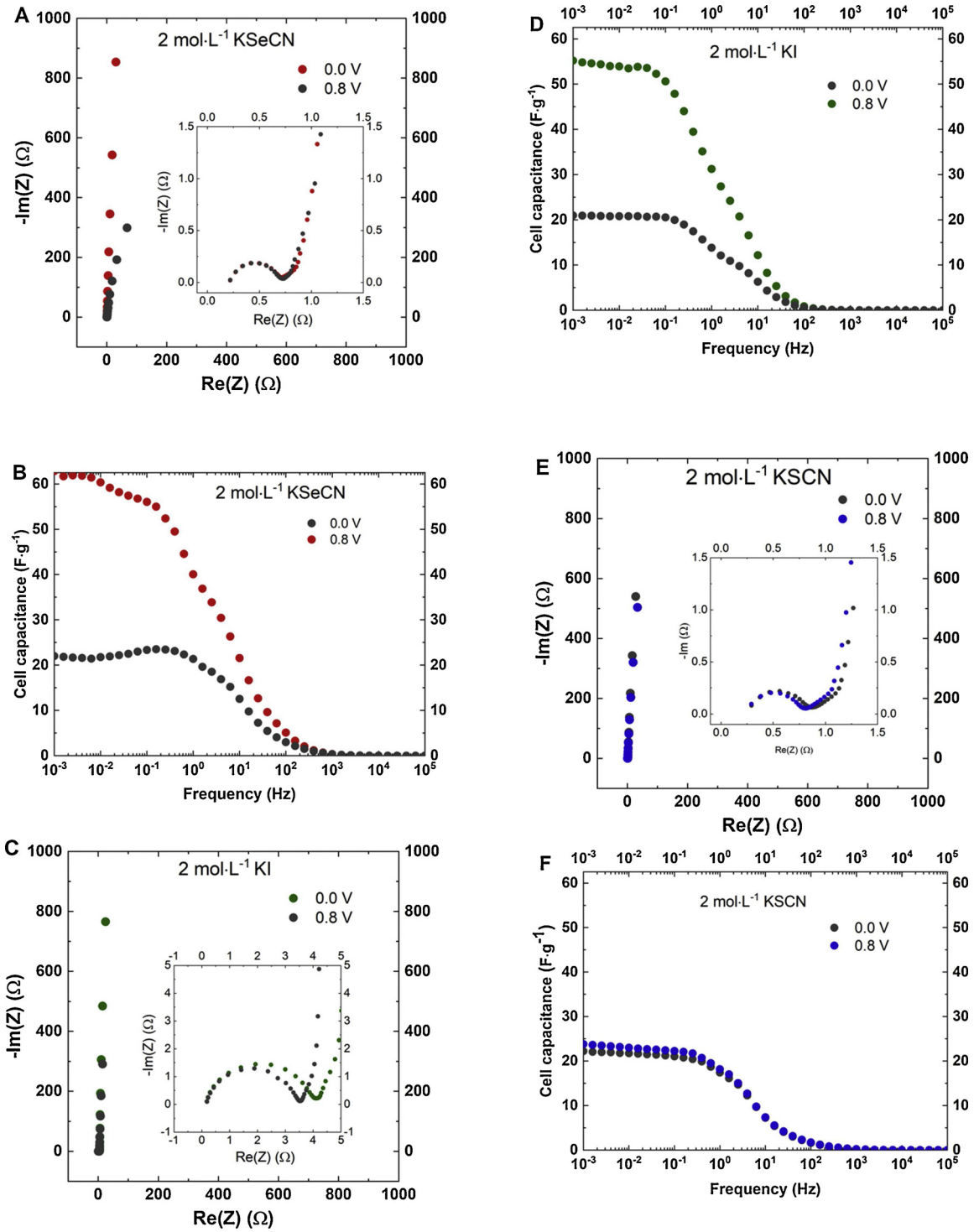

Fig. 4. Nyquist plots for 2 mol·L^{-1} solutions (a) KSeCN (c) KI (e) KSCN and capacitance in function of frequency (b) KSeCN, (d) KI, (f) KSCN in the frequency range 1 mHz to 100 kHz.

process is limited by diffusion (linear trend) or by reaction kinetics (non-linear dependence). Taking into consideration the values corresponding to the current loading in the range of 0.5 ÷ 5 A·g^{-1}, the dependence is linear – indicating a limited diffusion process. In turn, at 10 A·g^{-1} the process limited by kinetics is assumed. Besides, based on the calculated energy efficiencies (Table 2), the highest reversibility was observed for 0.5 and 1 A·g^{-1} current load. Further increase in current densities resulted in a gradual decrease in energy efficiency – down to 32% for 10 A·g^{-1} for KSeCN. It means that the higher current density, the worse reversibility of the redox processes occurring at this system $SeCN^{-}/(SeCN)_2$ which definitely proves the redox-originating capacity in the system. Coulombic efficiency increases with current density, and for 10 A·g^{-1} reaches an artificial value of 130% (!!!). Certainly, such a value cannot be considered as correct one (max. 100%), however, it indicates that additional reactions of various origin can occur in the system. At such high current load conditions, one should pay particular attention to the ohmic drop, since it might also affect the calculations. Finally, such result clearly demonstrates that the coulombic efficiency

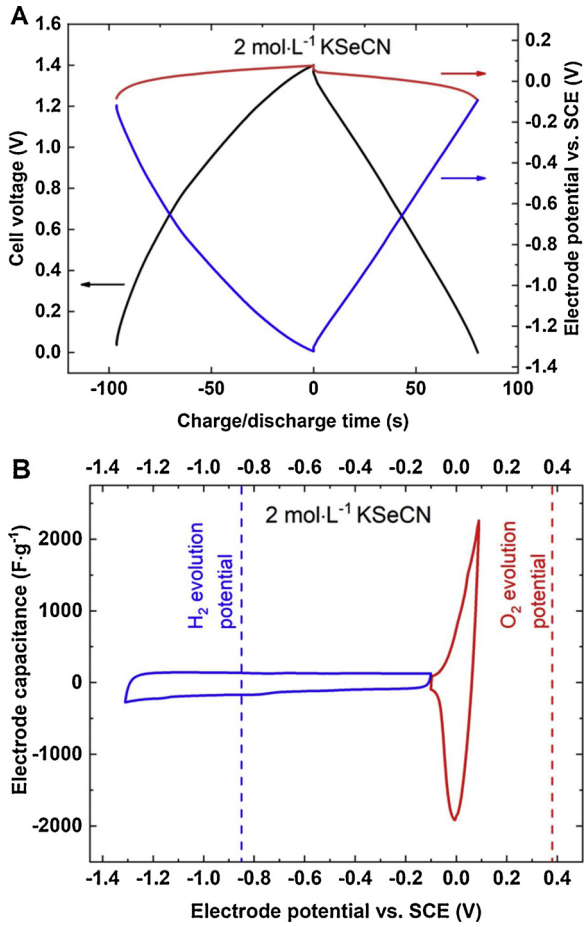

Fig. 5. (a) Galvanostatic charge/discharge profiles of full cell and electrodes (0.5 A·g^{-1}); (b) cyclic voltammetry profiles for the negative and positive electrode.

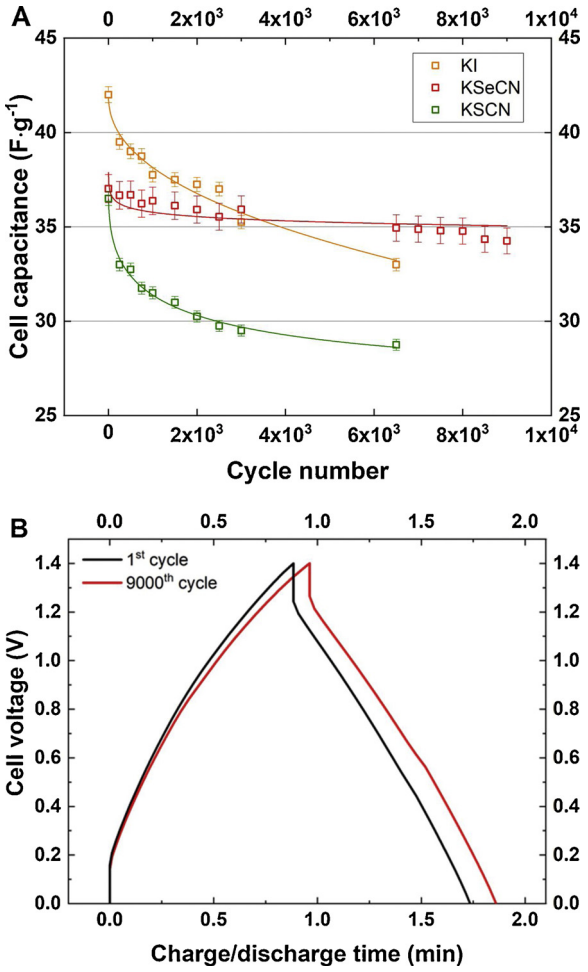

Fig. 6. (a) Capacitance vs. cycle number for 2 mol·L KI, KSeCN and KSCN-based systems (1 A·g^{-1}, U_{max} = 1.4 V) and (b) galvanostatic charge/discharge profiles (1 A·g^{-1}) for the first and the last cycle for KSeCN-based system.

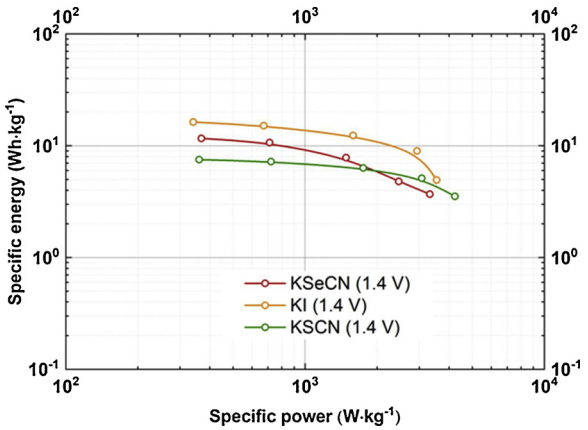

Fig. 7. Comparative Ragone plot for ECs with various electrolytes (calculated per active mass in the device).

is not the most reliable way to evaluate charge/discharge efficiency when the redox reactions are involved in the system's performance.

Fig. 4 compares the Nyquist plots for discharged (0 V) and charged (0.8 V) capacitors operating with 2 mol·L^{-1} (a) KSeCN, (c) KI and (e) KSCN electrolytes. The inset of the semi-circle on Nyquist plots demonstrates impeded charge transfer for KI solution (higher value of the real part of the impedance) contrarily to the systems operating with pseudohalide-based electrolytes. For discharged cells, the imaginary part of the impedance is almost vertical in all the cases. For charged systems (0.8 V), it is reduced noticeably in the case of ECs based on selenocyanate and iodide salts, evidencing their high redox-capacity. In the case of thiocyanate salt, imaginary parts of impedance are comparable at 0 V and 0.8 V. It is substantiated in a plot of capacitance vs. frequency (Fig. 4d–f). For charged ECs (0.8 V), the capacitance values are high at low-to-moderate frequencies, i.e., at 1 mHz: 63 F·g^{-1} for KSeCN and 56 F·g^{-1} for KI, whereas for discharged cells these values are definitely lower – around 23 F·g^{-1}. For KSCN-based cells, the capacitance values were comparable at 0 and 0.8 V. It again reflects a high formal potential of $SCN^-/(SCN)_2$ redox couple (E° = 0.77 V), demonstrating additional non-capacitive current at higher voltages. This comparison proves that selenocyanate and iodide-based electrolytes display a similar behavior because of their similar standard potentials in contrast to thiocyanate salt.

Taking into consideration the capacitance vs. frequency dependence for all electrolytes studied, one should notice that the cell voltage applied for electrochemical impedance measurements is an important parameter, essentially for the devices operating with redox-active electrolytes. It can be easily seen that capacitance "varies" significantly with the voltage applied. For this reason, caution shall be taken when reporting the capacitance values calculated from the impedance measurements. In our opinion, that value must absolutely be compared with those obtained by other techniques and the cell voltage applied must be clearly indicated.

In order to elucidate the performance of EC based on 2 mol·L^{-1} KSeCN, three-electrode experiments were carried out. Fig. 5a presents galvanostatic charge/discharge profiles of the full cell (1.4 V; black

Table 3
Leakage currents and self-discharge data for capacitor operating with 2 mol·L^{-1} KSeCN electrolyte.

Cell voltage (V)	Leakage current (A·g^{-1})	Cell voltage (V) at Open Circuit conditions	
		After 1 h	After 6 h
1.0	0.03	0.4	0.4
1.2	0.05	0.6	0.4
1.4	0.3	0.8	0.4
1.6	0.7	1.0	0.4

curve) and for single electrodes. The positive electrode (red curve) operates in a very narrow potential range (from -0.09 V to +0.07 V vs. SCE), whereas negative one (blue curve) operates in a wide potential range (from –0.09 V to −1.3 V vs. SCE). Such EC performance resembles an operation of capacitors based on iodide-containing electrolyte [95,112]. The cyclic voltammetry profiles for positive and negative electrode are shown in Fig. 5b.

The negative electrode exhibits shape typical of EDL charging with constant capacitance in the entire potential range. Positive electrode demonstrates huge "capacitance" originating from the activity of $SeCN^-/(SeCN)_2$ redox couple. However, such kind of profile cannot be considered either as capacitive nor pseudocapacitive and should not be presented in capacitance units. This is perfect evidence of the hybrid charge storage mechanism. Additionally, in contrast to KSCN electrolyte, where the asymmetric construction is necessary to take full advantage of thiocyanate/thiocyanogen redox couple [130], the device with KSeCN solution benefits from the faradaic contribution in a symmetric configuration. As anticipated, slightly alkaline pH shifted the electrode potentials towards lower values. As a result, the positive electrode operates far from E_{O2}, whereas the negative one demonstrates high overpotential for hydrogen evolution and operates far beyond E_{H2}.

Cyclability test (Fig. 6) evidences that the system is stable for at least 9 000 cycles at 1.4 V and less than 10% of capacitance loss is detected (37 F·g^{-1} for the first cycle and 34 F·g^{-1} for 9 000th cycle).

Based on the approximate calculations, the expected lifetime for this system is ca. 30 000 cycles. Galvanostatic charge/discharge curves (Fig. 6b) do not show significant deterioration in performance but the ohmic drop slightly increases. It demonstrates that EC based on 2 mol·L^{-1} KSeCN can operate at a voltage higher than for device with 2 mol·L^{-1} NaI [112], KSCN or KI. Additionally, no shift of the electrode potentials is observed using KSeCN electrolyte, contrarily to the device with NaI solution, where during cycling the faradaic contribution takes place also at the negative electrode. In this place it is worth to mention that comparisons of the cyclability tests should be made with special attention to the voltage and current load applied, essentially for the systems with a redox-based contribution. Certainly, the role of the electrode material applied cannot be neglected.

The Ragone plot (Fig. 7) compares the performance of ECs operating with 2 mol·L^{-1} KSeCN, KI and KSCN solutions.

It seems that KSeCN electrolyte allows more energy to be stored than in device with KSCN solution, but the power is negligibly lower. To some extent, this illustrates a "compromise" in energy and power enhancement. Although the energy is the highest for KI-based device, at 1.4 V capacitor voltage, the cyclability test results are in favor of KSeCN device.

Final evaluation of the proposed systems should concern the leakage current and self-discharge measurements. Leakage current should be measured for at least 2 h during potentiostatic hold at a certain voltage. Self-discharge should be monitored at least for 6 h or until the voltage drop is less than 10 mV·h^{-1}.

Data presented in Table 3 indicate that the capacitors with redox-active electrolyte suffer from high leakage current and fast self-discharge, once the potential redox activity is reached (in the considered case, above 1.2 V). It means that the energy accumulated is high, but the dissipation occurs quite quickly. This phenomenon originates most likely from two different mechanisms of charge storage (capacitive and faradaic), combined in one device.

4. Conclusions

This study demonstrates the operation of the electrochemical capacitor based on a novel redox active electrolyte. The 2 mol·L^{-1} KSeCN solution displays high conductivity (194 mS·cm^{-1}) and slightly alkaline pH (10.33). Owing to the low standard potential of $SeCN^-/(SeCN)_2/(SeCN)_3^-$ redox system, the positive electrode is dominated by faradaic contribution whereas negative one performs by electric double layer charging. Using economically reasonable stainless steel current collectors, the capacitor demonstrates high capacitance (43 F·g^{-1} at 0.5 A·g^{-1}), reasonable operational voltage (1.4 V) and long cycle life. The leakage current and self-discharge at elevated voltages rates must be a subject of further improvement.

Acknowledgements

Authors acknowledge European Research Council (ERC) for funding provided within ERC-StG-2017 project (GA 759603) under the European Union's Horizon 2020 research and innovation programme.

References

[1] F. Beguin, V. Presser, A. Balducci, E. Frackowiak, Adv. Mater. 26 (2014) 2219–2251.
[2] A. Gonzalez, E. Goikolea, J.A. Barrena, R. Mysyk, Renew. Sust. Energy Rev. 58 (2016) 1189–1206.
[3] J.R. Miller, IEEE Electr. Insul. Mag. 26 (2010) 40–47.
[4] A. Slesinski, J.R. Miller, F. Beguin, E. Frackowiak, J. Electrochem. Soc. 164 (2017) A2732–A2737.
[5] J.R. Miller, A.F. Burke, Electrochem. Soc. Interface 17 (2008) 53–57.
[6] A. Burke, Electrochim. Acta 53 (2007) 1083–1091.
[7] M. Halper, J. Ellenbogen, Report No. MP 05W0000272, (2006), pp. 1–29.
[8] M. Jayalakshmi, K. Balasubramanian, in, 2008, pp. 1196-1217.
[9] J. Ho, T.R. Jow, S. Boggs, IEEE Electr. Insul. Mag. 26 (2010) 20–25.
[10] P. Sharma, T.S. Bhatti, Energy Convers. Manage. 51 (2010) 2901–2912.
[11] N.S. Choi, Z. Chen, S.A. Freunberger, X. Ji, Y.K. Sun, K. Amine, G. Yushin, L.F. Nazar, J. Cho, P.G. Bruce, Angew. Chem. Int. Ed. Engl. 51 (2012) 9994–10024.
[12] C.R. Dennison, V. Presser, J. Campos, K.W. Knehr, E.C. Kumbur, Y. Gogotsi, Abstr. Pap. Am. Chem. Sci. 244 (2012).
[13] A. Yu, Electrochemical Supercapacitors for Energy Storage and Delivery Fundamentals and Applications, (2013).
[14] K. Naoi, Electrochemistry 81 (2013) 775–776.
[15] K. Naoi, Y. Nagano, W. Naoi, Carbon 57 (2013) 539-539.
[16] K. Naoi, W. Naoi, S. Aoyagi, J. Miyamoto, T. Kamino, ACC. Chem. Res. 46 (2013) 1075–1083.
[17] P. Kurzweil, Electrochemical double-layer capacitors, Electrochemical Energy Storage for Renewable Sources and Grid Balancing, (2015), pp. 345–407.
[18] C. Zhong, Y. Deng, W. Hu, J. Qiao, L. Zhang, J. Zhang, Chem. Soc. Rev. 44 (2015) 7484–7539.
[19] N. Choudhary, C. Li, J. Moore, N. Nagaiah, L. Zhai, Y. Jung, J. Thomas, Adv. Mater. 29 (2017) 1605336-n/a.
[20] W. Zuo, R. Li, C. Zhou, Y. Li, J. Xia, J. Liu, Adv. Sci. (Weinh) 4 (2017) 1600539.
[21] M. Winter, R.J. Brodd, Chem. Rev. 104 (2004) 4245–4270.
[22] E. Lust, A. Janes, M. Arulepp, J. Electroanal. Chem. 562 (2004) 33–42.
[23] M. Arulepp, L. Permann, J. Leis, A. Perkson, K. Rumma, A. Janes, E. Lust, J. Power Sources 133 (2004) 320–328.
[24] Y.J. Kim, Y. Horie, S. Ozaki, Y. Matsuzawa, H. Suezaki, C. Kim, N. Miyashita, M. Endo, Carbon 42 (2004) 1491–1500.
[25] O. Barbieri, M. Hahn, A. Herzog, R. Kotz, Carbon 43 (2005) 1303–1310.
[26] T.A. Centeno, M. Sevilla, A.B. Fuertes, F. Stoeckli, Carbon 43 (2005) 3012–3015.
[27] L.H. Wang, M. Fujita, M. Inagaki, Electrochim. Acta 51 (2006) 4096–4102.
[28] E. Raymundo-Pinero, K. Kierzek, J. Machnikowski, F. Beguin, Carbon 44 (2006) 2498–2507.
[29] G. Salitra, A. Soffer, L. Eliad, Y. Cohen, D. Aurbach, J. Electrochem. Soc. 147 (2000) 2486–2493.
[30] C. Vix-Guterl, S. Saadallah, K. Jurewicz, E. Frackowiak, M. Reda, J. Parmentier, J. Patarin, F. Beguin, Mat. Sci. Eng. B-Solid 108 (2004) 148–155.
[31] M.J. Bleda-Martinez, J.A. Macia-Agullo, D. Lozano-Castello, E. Morallon, D. Cazorla-Amoros, A. Linares-Solano, Carbon 43 (2005) 2677–2684.
[32] C. Vix-Guterl, E. Frackowiak, K. Jurewicz, M. Friebe, J. Parmentier, F. Beguin, Carbon 43 (2005) 1293–1302.

[33] A.G. Pandolfo, A.F. Hollenkamp, J. Power Sources 157 (2006) 11–27.
[34] F. Beguin, R. Yazami, Actual. Chim. (2006) 86–90.
[35] F. Beguin, J. Braz. Chem. Soc. 17 (2006) 1083–1089.
[36] M. Inagaki, M. Toyoda, Y. Soneda, S. Tsujimura, T. Morishita, in, 2016, pp. 448-473.
[37] B. Lobato, L. Suarez, L. Guardia, T.A. Centeno, Carbon 122 (2017) 434–445.
[38] A. Vlad, A. Balducci, Nat. Mater. 16 (2017) 161–162.
[39] M. Mirzaeian, Q. Abbas, A. Ogwu, P. Hall, M. Goldin, M. Mirzaeian, H.F. Jirandehi, Int. J. Hydrogen Energy 42 (2017) 25565–25587.
[40] K. Fic, A. Platek, J. Piwek, E. Frackowiak, Mater. Today 21 (2018) 437–454.
[41] F. Béguin, E. Frąckowiak, Carbons for Electrochemical Energy Storage and Conversion Systems, CRC Press, New York, 2009.
[42] F. Béguin, E. Frąckowiak, Supercapacitors, Wiley-VCH Verlag GmbH & Co. KGaA, Weinheim, Germany, 2013.
[43] W.T. Gu, G. Yushin, Wires Energy Environ. 3 (2014) 424–473.
[44] M. Sevilla, R. Mokaya, Energy Environ. Sci. 7 (2014) 1250–1280.
[45] Y. Gogotsi, D. Guldi, R. McCreery, C.C. Hu, C. Merlet, F. Beguin, L. Hardwick, E. Frackowiak, J. Macpherson, A. Forse, G.Z. Chen, K. Holt, R. Dryfe, H. Kurig, S. Sharma, P.R. Unwin, T. Rabbow, W. Yu, F. Qiu, F. Juarez, C. Sole, B. Dyatkin, K. Stevenson, Y. Cao, N. Cousens, A. Noofeli, Faraday Discuss. 172 (2014) 239–260.
[46] Y. Zhao, Z. Song, X. Li, Q. Sun, N. Cheng, S. Lawes, X. Sun, Energy Storage Mater. 2 (2016) 35–62.
[47] H. Lu, X.S. Zhao, Sustain. Energy Fuels 1 (2017) 1265–1281.
[48] F. Stoeckli, T.A. Centeno, Carbon 43 (2005) 1184–1190.
[49] T.A. Centeno, O. Sereda, F. Stoeckli, Phys. Chem. Chem. Phys. 13 (2011) 12403–12406.
[50] F. Stoeckli, T.A. Centeno, Phys. Chem. Chem. Phys. 14 (2012) 11589–11591.
[51] F. Stoeckli, T.A. Centeno, J. Mater. Chem. A 1 (2013) 6865–6873.
[52] D. Weingarth, H. Noh, A. Foelske-Schmitz, A. Wokaun, R. Kotz, Electrochim. Acta 103 (2013) 119–124.
[53] A. Balducci, J. Power Sources 326 (2016) 534–540.
[54] M.P. Mousavi, B.E. Wilson, S. Kashefolgheta, E.L. Anderson, S. He, P. Buhlmann, A. Stein, ACS Appl. Mater. Interfaces 8 (2016) 3396–3406.
[55] C. Zhong, Y. Deng, W. Hu, D. Sun, X. Han, J. Qiao, J. Zhang, Electrolytes for Electrochemical Supercapacitors, CRC Press, New York, 2016.
[56] D.R. MacFarlane, M. Forsyth, P.C. Howlett, M. Kar, S. Passerini, J.M. Pringle, H. Ohno, M. Watanabe, F. Yan, W.J. Zheng, S.G. Zhang, J. Zhang, Nat. Rev. Mater. 1 (2016).
[57] M. Salanne, Top. Curr. Chem. 375 (2017) 63–69.
[58] X.H. Wang, Y.H. Li, F.L. Lou, M.E.M. Buan, E. Sheridan, D. Chen, RSC Adv. 7 (2017) 23859–23865.
[59] X. Wang, A.Y. Mehandzhiyski, B. Arstad, K.L. Van Aken, T.S. Mathis, A. Gallegos, Z. Tian, D. Ren, E. Sheridan, B.A. Grimes, D.E. Jiang, J. Wu, Y. Gogotsi, Chen, J. Am. Chem. Soc. 139 (2017) 18681–18687.
[60] Y. Yamada, Electrochemistry 85 (2017) 559–565.
[61] Y. Yamada, A. Yamada, Chem. Lett. 46 (2017) 1056–1064.
[62] S. Uchida, M. Ishikawa, J. Power Sources 359 (2017) 480–486.
[63] B. Gorska, L. Timperman, M. Anouti, F. Beguin, Phys. Chem. Chem. Phys. 19 (2017) 11173–11186.
[64] B. Dyatkin, N.C. Osti, Y. Zhang, Y. Zhang, H.W. Wang, E. Mamontov, W.T. Heller, P.F. Zhang, G. Rother, P.T. Cummings, D.J. Wesolowski, Y. Gogotsi, Carbon 129 (2018) 104–118.
[65] N. Hirota, K. Okuno, M. Majima, A. Hosoe, S. Uchida, M. Ishikawa, Electrochim. Acta 276 (2018) 125–133.
[66] J. Krummacher, C. Schutter, L.H. Hess, A. Balducci, Curr Opin Electroche 9 (2018) 64–69.
[67] V. Ruiz, R. Santamaria, M. Granda, C. Blanco, Electrochim. Acta 54 (2009) 4481–4486.
[68] L. Demarconnay, E. Raymundo-Pinero, F. Beguin, Electrochem. Commun. 12 (2010) 1275–1278.
[69] M.P. Bichat, E. Raymundo-Pinero, F. Beguin, Carbon 48 (2010) 4351–4361.
[70] K. Fic, G. Lota, M. Meller, E. Frackowiak, Energy Environ. Sci. 5 (2012) 5842–5850.
[71] Q. Gao, L. Demarconnay, E. Raymundo-Pinero, F. Beguin, Energy Environ. Sci. 5 (2012) 9611–9617.
[72] P. Ratajczak, K. Jurewicz, P. Skowron, Q. Abbas, F. Beguin, Electrochim. Acta 130 (2014) 344–350.
[73] I.M. Svishchev, R.A. Carvajal-Ortiz, K.I. Choudhry, D.A. Guzonas, Corros. Sci. 72 (2013) 20–25.
[74] Q. Abbas, P. Ratajczak, F. Beguin, Faraday Discuss. 172 (2014) 199–214.
[75] P. Ratajczak, K. Jurewicz, F. Beguin, J. Appl. Electrochem. 44 (2014) 475–480.
[76] K. Soeda, M. Yamagata, M. Ishikawa, A. Manivannan, S. Mukerjee, B.Y. Liaw, M. Doeff, D. Wang, J. Xiao (Eds.), Electrochemical Society Inc. 2015, pp. 13–22.
[77] J. Wojciechowski, K. Szubert, R. Peipmann, M. Fritz, U. Schmidt, A. Bund, G. Lota, Electrochim. Acta 220 (2016) 1–10.
[78] K. Szubert, J. Wojciechowski, J. Karasiewicz, H. Maciejewski, G. Lota, Int. J. Electrochem. Sci. 11 (2016) 8256–8269.
[79] M.L. He, K. Fic, E. Frackowiak, P. Novak, E.J. Berg, Energy Environ. Sci. 9 (2016) 623–633.
[80] J. Wojciechowski, L. Kolanowski, A. Bund, G. Lota, J. Power Sources 368 (2017) 18–29.
[81] P. Simon, Y. Gogotsi, B. Dunn, Science 343 (2014) 1210–1211.
[82] T. Brousse, D. Bélanger, J.W. Long, J. Electrochem. Soc. 162 (2015) A5185–A5189.
[83] L. Guan, L.P. Yu, G.Z. Chen, Electrochim. Acta 206 (2016) 464–478.
[84] B. Akinwolemiwa, C. Peng, G.Z. Chen, J. Electrochem. Soc. 162 (2015) A5054–A5059.
[85] S. Roldan, D. Barreda, M. Granda, R. Menendez, R. Santamaria, C. Blanco, Phys. Chem. Chem. Phys. 17 (2015) 1084–1092.
[86] S. Trasatti, P. Kurzweil, Platin. Met. Rev. 38 (1994) 46–56.
[87] B.E. Conway, V. Birss, J. Wojtowicz, J. Power Sources 66 (1997) 1–14.
[88] B.E. Conway, Similarities and differences between supercapacitors and batteries for storing electrical energy, Electrochemical Supercapacitors, (1999), pp. 11–31.
[89] B.E. Conway, W.G. Pell, J. Solid State Electrochem. 7 (2003) 637–644.
[90] T. Cottineau, M. Toupin, T. Delahaye, T. Brousse, D. Belanger, Appl Phys a-Mater 82 (2006) 599–606.
[91] G.A. Snook, P. Kao, A.S. Best, J. Power Sources 196 (2011) 1–12.
[92] C. Costentin, T.R. Porter, J.-M. Savéant, ACS Appl. Mater. Interfaces 9 (2017) 8649–8658.
[93] P.R. Bueno, J. Power Sources 414 (2019) 420–434.
[94] A. Balducci, D. Belanger, T. Brousse, J.W. Long, W. Sugimoto, J. Electrochem. Soc. 164 (2017) A1487–A1488.
[95] G. Lota, E. Frackowiak, Electrochem. Commun. 11 (2009) 87–90.
[96] G. Lota, K. Fic, E. Frackowiak, Electrochem. Commun. 13 (2011) 38–41.
[97] M. Meller, K. Fic, J. Menzel, E. Frackowiak, Phys. Chem. Electrolytes 61 (2014) 1–8.
[98] K.W. Leitner, B. Gollas, M. Winter, J.O. Besenhard, Electrochim. Acta 50 (2004) 199–204.
[99] T. Tomai, S. Mitani, D. Komatsu, Y. Kawaguchi, I. Honma, Sci. Rep. 4 (2014) 3591-3591.
[100] Y.F. Nie, Q. Wang, X.Y. Chen, Z.J. Zhang, Phys. Chem. Chem. Phys. 18 (2016) 2718–2729.
[101] G. Pognon, T. Brousse, D. Belanger, Carbon 49 (2011) 1340–1348.
[102] G. Pognon, T. Brousse, L. Demarconnay, D. Belanger, J. Power Sources 196 (2011) 4117–4122.
[103] G. Pognon, C. Cougnon, D. Mayilukila, D. Belanger, ACS Appl. Mater. Interaces 4 (2012) 3788–3796.
[104] M. Weissmann, O. Crosnier, T. Brousse, D. Belanger, Electrochim. Acta 82 (2012) 250–256.
[105] A. Le Comte, G. Pognon, T. Brousse, D. Bélanger, Electrochemistry 81 (2013) 863–866.
[106] A. Le Comte, T. Brousse, D. Bélanger, Electrochim. Acta 137 (2014) 447–453.
[107] A. Le Comte, D. Chhin, A. Gagnon, R. Retoux, T. Brousse, D. Bélanger, J. Mater. Chem. A 3 (2015) 6146–6156.
[108] S. Roldan, C. Blanco, M. Granda, R. Menendez, R. Santamaria, Angew. Chem. Int. Ed. Engl. 50 (2011) 1699–1701.
[109] S. Roldan, M. Granda, R. Menendez, R. Santamaria, C. Blanco, J. Phys. Chem. C 115 (2011) 17606–17611.
[110] E. Frackowiak, M. Meller, J. Menzel, D. Gastol, K. Fic, Faraday Discuss. 172 (2014) 179–198.
[111] S.T. Senthilkumar, R.K. Selvan, Y.S. Lee, J.S. Melo, J. Mater. Chem. A 1 (2013) 1086–1095.
[112] J. Menzel, K. Fic, M. Meller, E. Frackowiak, J. Appl. Electrochem. 44 (2014) 439–445.
[113] X. Wang, R.S. Chandrabose, S.E. Chun, T. Zhang, B. Evanko, Z. Jian, S.W. Boettcher, G.D. Stucky, X. Ji, ACS Appl. Mater. Interfaces 7 (2015) 19978–19985.
[114] S. Roldán, Z. González, C. Blanco, M. Granda, R. Menéndez, R. Santamaría, Electrochim. Acta 56 (2011) 3401–3405.
[115] S. Roldán, M. Granda, R. Menéndez, R. Santamaría, C. Blanco, Electrochim. Acta 83 (2012) 241–246.
[116] H.J. Yu, L.Q. Fan, J.H. Wu, Y.Z. Lin, M.L. Huang, J.M. Lin, Z. Lan, RSC Adv. 2 (2012) 6736–6740.
[117] J.H. Wu, H.J. Yu, L.Q. Fan, G.G. Luo, J.M. Lin, M.L. Huang, J. Mater. Chem. 22 (2012) 19025–19030.
[118] P. Díaz, Z. González, R. Santamaría, M. Granda, R. Menéndez, C. Blanco, Electrochim. Acta 168 (2015) 277–284.
[119] K. Fic, M. Meller, E. Frackowiak, Electrochim. Acta 128 (2014) 210–217.
[120] S.E. Chun, B. Evanko, X. Wang, D. Vonlanthen, X. Ji, G.D. Stucky, S.W. Boettcher, Nat. Commun. 6 (2015) 7818.
[121] S. Sathyamoorthi, M. Kanagaraj, M. Kathiresan, V. Suryanarayanan, D. Velayutham, J. Mater. Chem. A 4 (2016) 4562–4569.
[122] K. Fic, M. Meller, E. Frackowiak, J. Electrochem. Soc. 162 (2015) A5140–A5147.
[123] A. Kolodziej, K. Fic, E. Frackowiak, J. Mater. Chem. A 3 (2015) 22923–22930.
[124] Q. Abbas, F. Beguin, Prog. Nat. Sci.-Mater. 25 (2015) 622–630.
[125] J. Menzel, K. Fic, E. Frackowiak, Prog. Nat. Sci.-Mater. 25 (2015) 642–649.
[126] E. Frackowiak, K. Fic, M. Meller, G. Lota, ChemSusChem 5 (2012) 1181–1185.
[127] S.T. Senthilkumar, R.K. Selvan, J.S. Melo, J. Mater. Chem. A 1 (2013) 12386–12394.
[128] K. Jurewicz, E. Frackowiak, F. Beguin, Appl. Phys. a-Mater. 78 (2004) 981–987.
[129] S.E. Chun, J.F. Whitacre, J. Power Sources 242 (2013) 137–140.
[130] B. Gorska, P. Bujewska, K. Fic, Phys. Chem. Chem. Phys. 19 (2017) 7923–7935.
[131] G. Oskam, B.V. Bergeron, G.J. Meyer, P.C. Searson, J. Phys. Chem. B 105 (2001) 6867–6873.
[132] B.V. Bergeron, A. Marton, G. Oskam, G.J. Meyer, J. Phys. Chem. B 109 (2005) 937–943.
[133] P. Wang, S.M. Zakeeruddin, J.E. Moser, R. Humphry-Baker, M. Gratzel, J. Am. Chem. Soc. 126 (2004) 7164–7165.
[134] A. Solangi, A.M. Bond, I. Burgar, A.F. Hollenkamp, M.D. Horne, T. Ruther, C. Zhao, J. Phys. Chem. B 115 (2011) 6843–6852.
[135] F. Bella, A. Sacco, G.P. Salvador, S. Bianco, E. Tresso, C.F. Pirri, R. Bongiovanni, J.

Phys. Chem. C 117 (2013) 20421–20430.
[136] C.L. Bentley, A.M. Bond, A.F. Hollenkamp, P.J. Mahon, J. Zhang, J. Phys. Chem. C 119 (2015) 21828–21839.
[137] C.T. Li, C.P. Lee, C.T. Lee, S.R. Li, S.S. Sun, K.C. Ho, ChemSusChem 8 (2015) 1244–1253.
[138] P. Krishnan, J. Solid State Electrochem. 11 (2007) 1327–1334.
[139] M.E. Martins, C.E. Castellano, A.J. Calandra, A.J. Arvia, Anal. Chem. 50 (2002) 229–231.
[140] J. Jagiello, J.P. Olivier, J. Phys. Chem. C 113 (2009) 19382–19385.
[141] J. Jagiello, J.P. Olivier, Adsorpt.-J. Int. Adsorpt. Soc. 19 (2013) 777–783.
[142] J. Jagiello, J.P. Olivier, Carbon 55 (2013) 70–80.
[143] K. Fic, M. Meller, J. Menzel, E. Frackowiak, Electrochim. Acta 206 (2016) 496–503.